Measurement-Based Estimation of Linear Sensitivity Distribution Factors and Applications

Yu Christine Chen *Student Member, IEEE*, Alejandro D. Domínguez-García *Member, IEEE*, and
Peter W. Sauer *Life Fellow, IEEE*

Abstract—In this paper, we propose a method to compute linear sensitivity distribution factors (DFs) in near real-time. The method does not rely on the system power flow model. Instead, it uses only high-frequency synchronized data collected from phasor measurement units to estimate the injection shift factors through linear least-squares estimation, after which other DFs can be easily computed. Such a measurement-based approach is desirable since it is adaptive to changes in system operating point and topology. We further improve the adaptability of the proposed approach to such changes by using weighted and recursive least-squares estimation. Through numerical examples, we illustrate the advantages of our proposed DF estimation approach over the conventional model-based one in the context of contingency analysis and generation re-dispatch.

I. Introduction

In order to monitor and maintain operational reliability, power system operators perform several static security analyses. For example, the results of online N-1 contingency analysis help operators determine whether or not the system will meet operational reliability requirements in case of outage in any one particular asset (e.g., a generator or a transmission line), and further whether or not corrective actions, such as generation re-dispatch in a constrained system, are required [1], [2]. These studies may include repeated computations, for each credible contingency, of power flow solutions using the full nonlinear power flow model or a linearized model. To reduce the computational burden of evaluating repeated power flow solutions, linear sensitivity distribution factors (DFs), such as injection shift factors (ISFs), power transfer distribution factors (PTDFs), and line outage distribution factors (LODFs), are used to predict the effect of an operating point change on the system [3]. For example, in the context of N-1 contingency analysis, ISFs and LODFs are utilized, in conjunction with an estimate of the system's current operating point, to predict the change in power flowing through transmission lines in the event that an outage in certain generating facilities or transmission lines occurs [3]. These predictions are then used to determine whether or not any line loading limits would be violated. In general, these online studies require the maintenance of up-to-date and accurate internal system model and external balancing area equivalents.

Conventional model-based studies are not ideal since the results depend on an accurate model with up-to-date network topology, which may not be available due to erroneous telemetry from remotely monitored circuit breakers. For example, in the 2011 San Diego blackout, operators could not detect that certain lines were overloaded or close to being overloaded because the network model was not up-to-date [1]. Furthermore, the results from model-based studies may not be applicable if the actual system evolution does not match any predicted operating points due to unforeseen circumstances such as equipment failure, large variations in generation or load, or unpredictable levels of renewable generation. Thus, conventional model-based techniques may no longer satisfy the needs of monitoring and protection tasks and therefore, it is important to develop power system monitoring tools that are adaptive to changes in operating point and topology. In this regard, phasor measurement units (PMUs) are an enabling technology for the development of such measurement-based monitoring tools.

Unlike current system measurements, PMUs measure voltages, currents, and frequency at a very high speed (usually 30 measurements per second) [4], and phasors measured at different locations by different devices are time-synchronized [5]. In this paper, we propose a method to estimate linear sensitivity DFs that exploits measurements obtained from PMUs in near real-time without the use of a power flow model of the system. In particular, we rely on real power bus injection and line flow data obtained from PMUs, and the small fluctuations inherent to load and generation to compute the linear sensitivity DFs through the solution of a linear least-squares estimation (LSE) problem.

Linear sensitivity DFs are widely known and used in power systems analyses [3], [6]. Existing approaches to computing DFs typically employ so-called DC approximations, which can provide fast contingency screening [7]. They do not, however, have the flexibility of adapting to changes in network topology or generation and load variations, which can all affect the actual linear sensitivities [8]. Recent attention has been given to the computation of the LODF due to their prominent role in revealing and ameliorating cascading outages [9], [10]. Additionally, work has been done in the area of detecting line outages using PMU measurements [11], [12]. Such proposed approaches still largely rely on a model of the system and utilize the so-called DC approximation. In [13], phasor measurements were used in online contingency analysis by monitoring buses that had been classified as high-risk by an offline study.

This paper builds on preliminary work reported in [14] and provides extensions in several directions. First, we utilize a weighted least-squares (WLS) framework to improve the adaptability of the proposed measurement-based approach by placing more weight on recent measurements and less on past ones. Second, since measurements would be acquired sequentially in a practical setting, we implement the least-squares estimator recursively so that the ISF estimates are refined through each additional set of measurements obtained. Further, we formulate two common power system analysis applications that use DFs, contingency analysis and generation re-dispatch, and showcase the advantages of the proposed measurement-based approach on the 118-bus IEEE system.

The remainder of this paper is organized as follows. Section II outlines the problem statement and describes the conventional model-based solution. In Section III, we formulate the proposed measurement-based estimation problem approach and provide several LSE-based algorithms to solve it; additionally, we show how to compute other DFs once ISF estimates are obtained. In Section IV, we describe the role of measurement-based DFs in several power systems analysis applications, illustrating them via examples involving the IEEE 14-bus system. In Section V, we demonstrate the proposed ideas via a case study involving the IEEE 118-bus system. Finally, in Section VI, we offer concluding remarks and directions for future research.

II. PRELIMINARIES

Distribution factors are linearized sensitivities used in, e.g., online contingency analysis, generation re-dispatch, and congestion relief [3]. A key distribution factor is the injection shift factor (ISF), which quantifies the redistribution of power through each transmission line following a change in generation or load on a particular bus with a slack bus constraint included. In essence, the ISF captures the sensitivity of the flow through a line with respect to changes in generation or load. Other DFs include the power transfer distribution factor (PTDF), the line outage distribution factor (LODF), and the outage transfer distribution factor (OTDF) [7], which can all be derived from the ISF.

Let $\mathcal{L}$ denote the set of transmission lines and $\mathcal{B}$ the set of buses in the system; the ISF of line $L_{k\text{-}l} \in \mathcal{L}$ (assume positive real power flow from bus k to l measured at bus k) with respect to bus $i \in \mathcal{B}$, which we denote by $\Psi_{k\text{-}l}^i$, is the linear approximation of the sensitivity of the active power flow in line $L_{k\text{-}l}$ with respect to the active power injection at bus i with the location of the slack bus specified and all other quantities constant. Suppose P_i varies by a small amount ΔP_i and denote by $\Delta P_{k\text{-}l}^i$ the change in active power flow in line $L_{k\text{-}l}$ (measured at bus k) resulting from ΔP_i. Then, it follows that

$$\Psi_{k\text{-}l}^i := \frac{\partial P_{k\text{-}l}}{\partial P_i} \approx \frac{\Delta P_{k\text{-}l}^i}{\Delta P_i}. \tag{1}$$

Traditionally, ISFs, along with other DFs, have been computed offline based on a model of the power system, including its topology and pertinent parameters. Next, we describe this model-based approach to compute ISFs and motivate the need for a measurement-based approach.

A. Model-Based Approach to ISF Computation

Consider a power system with n buses, and let V_i and θ_i, respectively, denote the voltage magnitude and angle at bus i; additionally, let P_i and Q_i, respectively, denote the active and reactive power injection (generator or load) at bus i. Then, the static behavior of a power system can be described by the power flow equations, which we write compactly as

$$g(x, P, Q) = 0, \tag{2}$$

where $x = [\theta_1, \ldots, \theta_n, V_1, \ldots, V_n]^T$, $P = [P_1, \ldots, P_n]^T$, $Q = [Q_1, \ldots, Q_n]^T$, and $g : \mathbb{R}^{2n} \times \mathbb{R}^n \times \mathbb{R}^n \to \mathbb{R}^{2n}$. In (2), the dependence on network parameters, such as line series and shunt impedances, is implicitly considered in the function $g(\cdot)$.

Suppose a solution for (2) is obtained at (x_0, P_0, Q_0), i.e., $g(x_0, P_0, Q_0) = 0$, and assume $g(\cdot)$ is continuously differentiable with respect to x and P at (x_0, P_0, Q_0). Let $x = x_0 + \Delta x$ and $P = P_0 + \Delta P$. Then, assuming that ΔP and Δx are sufficiently small, we can approximate $g(x, P, Q_0)$ as

$$g(x, P, Q_0) \approx g(x_0, P_0, Q_0) + J\Delta x + D\Delta P, \tag{3}$$

where

$$J = \frac{\partial g}{\partial x}\Big|_{(x_0, P_0, Q_0)} \text{ and } D = \frac{\partial g}{\partial P}\Big|_{(x_0, P_0, Q_0)}.$$

Since $g(x_0, P_0, Q_0) = 0$, and assume Δx and ΔP are small, we have that $g(x, P, Q_0) \approx 0$. Then, it follows from (3) that

$$0 \approx J\Delta x + D\Delta P. \tag{4}$$

Further, since J is the Jacobian of the power flow equations, which we assume to be invertible around (x_0, P_0, Q_0), we can rearrange (4) to obtain

$$\Delta x \approx -J^{-1}D\Delta P. \tag{5}$$

Next, we consider the active power flow through line $L_{k\text{-}l}$ as $P_{k\text{-}l} = h_{k\text{-}l}(x)$, where $h_{k\text{-}l} : \mathbb{R}^{2n} \to \mathbb{R}$. Under the same small Δx assumption, we can obtain an expression for small variations $\Delta P_{k\text{-}l}$ due to Δx as follows:

$$\Delta P_{k\text{-}l} = c\Delta x, \tag{6}$$

where $c = \frac{\partial h_{k\text{-}l}}{\partial x}\Big|_{x_0}$. Substituting (5) into (6), it follows that

$$\Delta P_{k\text{-}l} \approx -cJ^{-1}D\Delta P. \tag{7}$$

The derivation of the sensitivity vector $-cJ^{-1}D$ relies on the linearization of the nonlinear power flow equations around an operating point and therefore it depends on the system operating point.

For certain power system applications (such as congestion relief), the so-called DC assumptions are further used to simplify the AC linear sensitivities derived in (2)–(7) (see, e.g., [3]). Let $\tilde{B} = \text{diag}\{b_{k\text{-}l}\}$, a diagonal matrix whose entries are $b_{k\text{-}l}$, the susceptance of line $L_{k\text{-}l}$, for each $L_{k\text{-}l} \in \mathcal{L}$. Also, denote the line-to-bus incidence matrix by $A = [\ldots, a_{k\text{-}l}, \ldots]^T$, where $a_{k\text{-}l} \in \mathbb{R}^n$ is a vector in which the kth entry is 1 and the lth entry is -1. Then, by using the DC approximations [(i) the system is lossless, (ii) $V_i = 1$ p.u. for all $i \in \mathcal{B}$, and (iii) $\theta_i - \theta_j << 1$ for all $i, j \in \mathcal{B}$ [3]], the expression in (6) simplifies to

$$\Delta P_{k\text{-}l} \approx \tilde{B}_{k\text{-}l}AB^{-1}\Delta P, \tag{8}$$

where $\tilde{B}_{k\text{-}l}$ is the row in $\tilde{B}$ that corresponds to line $L_{k\text{-}l}$, and $B = A^T \tilde{B} A$. Then, by defining $\Psi_{k\text{-}l} = [\Psi_{k\text{-}l}^1, \ldots, \Psi_{k\text{-}l}^i, \ldots, \Psi_{k\text{-}l}^n]^T$, the model-based linear sensitivity factors for line $L_{k\text{-}l}$ with respect to active power injections at all buses are given by

$$\Psi_{k\text{-}l} = \tilde{B}_{k\text{-}l} A B^{-1}. \tag{9}$$

Under the DC assumptions, not only are the resulting DFs inflexible against variations in system topology, but they also remain constant through possible operating point variations under one topology, e.g., generation and load fluctuations.

B. Problem Statement

The conventional model-based approach to ISF computation outlined in (2)–(9) is not ideal since accurate and up-to-date network topology, parameters, and operating point are required. Moreover, under the DC assumptions, the model-based ISFs do not vary with system operating changes. In this paper, we aim to (i) eradicate the reliance on models for computing DFs and, (ii) improve adaptability of computed DFs to changes occurring in the system. With regard to this, we propose a method to estimate DFs using only PMU measurements obtained in near real-time without relying on a power flow model of the system.

III. MEASUREMENT-BASED DF COMPUTATION APPROACH

In this section, we formulate the proposed measurement-based method to compute the ISFs without relying on power flow models. Subsequently, we describe three LSE-based approaches to perform the computation. We illustrate the validity of our proposed measurement-based ISF computation approach in an example featuring the Western Electricity Coordinating Council (WECC) 3-machine 9-bus system. Finally, we describe steps to obtain other DFs, such as PTDFs, LODFs, and OTDFs, once the ISFs are computed.

A. ISF Computation

Let $P_i(t)$ denote the active power injection at bus i at time t; similarly, for $\Delta t > 0$ sufficiently small, let $P_i(t + \Delta t)$ denote the active power injection at time $t + \Delta t$. Define $\Delta P_i(t) = P_i(t + \Delta t) - P_i(t)$; then, based on the definition of the ISF in (1), we have that

$$\Psi_{k\text{-}l}^i \approx \frac{\Delta P_{k\text{-}l}^i(t)}{P_i(t + \Delta t) - P_i(t)}. \tag{10}$$

In order to obtain $\Psi_{k\text{-}l}^i$, we also need $\Delta P_{k\text{-}l}^i(t)$, which are not readily available from PMU measurements. We assume that the net variation in active power through line $L_{k\text{-}l}$, denoted by $\Delta P_{k\text{-}l}(t)$, however, is available. We express this net variation as the sum of active power variations in line $L_{k\text{-}l}$ due to active power injection variations at each bus i:

$$\Delta P_{k\text{-}l}(t) = \Delta P_{k\text{-}l}^1(t) + \cdots + \Delta P_{k\text{-}l}^n(t). \tag{11}$$

By substituting (10) into (11), we can rewrite (11) as

$$\Delta P_{k\text{-}l}(t) \approx \Delta P_1(t)\Psi_{k\text{-}l}^1 + \cdots + \Delta P_n(t)\Psi_{k\text{-}l}^n,$$

where $\Psi_{k\text{-}l}^i \approx \frac{\Delta P_{k\text{-}l}^i}{\Delta P_i}$, $i = 1, \ldots, n$. Suppose $m + 1$ sets of synchronized measurements are available. Let $\Delta P_i[j] = P_i((j + 1)\Delta t) - P_i(j\Delta t)$, and $\Delta P_{k\text{-}l}[j] = P_{k\text{-}l}((j + 1)\Delta t) - P_{k\text{-}l}(j\Delta t)$, $j = 1, \ldots, m$. Then, define $\Delta P_{k\text{-}l} = [\Delta P_{k\text{-}l}[1], \ldots, \Delta P_{k\text{-}l}[j], \ldots, \Delta P_{k\text{-}l}[m]]^T$, $\Delta P_i = [\Delta P_i[1], \ldots, \Delta P_i[j], \ldots, \Delta P_i[m]]^T$, and $\Psi_{k\text{-}l} = [\Psi_{k\text{-}l}^1, \ldots, \Psi_{k\text{-}l}^i, \ldots, \Psi_{k\text{-}l}^n]^T$. Further, suppose $m > n$, then we obtain the following overdetermined system:

$$\Delta P_{k\text{-}l} \approx \begin{bmatrix} \Delta P_1 & \cdots & \Delta P_i & \cdots & \Delta P_n \end{bmatrix} \Psi_{k\text{-}l}. \tag{12}$$

For ease of notation, let ΔP represent the $m \times n$ matrix $[\Delta P_1, \ldots, \Delta P_i, \ldots, \Delta P_n]$. Then, the system in (12) is of the form

$$\Delta P_{k\text{-}l} \approx \Delta P \Psi_{k\text{-}l}. \tag{13}$$

In (13), we hypothesize that the relationship between $\Delta P_{k\text{-}l}$ and $\Psi_{k\text{-}l}$ is approximately linear. Let $e \in \mathbb{R}^m$ denote the combination of inherent deterministic error arising from the linearization assumption and stochastic measurement error arising from faulty PMU data. As is customary, we assume the measurement error process is white with zero mean and variance σ^2 [15]. By explicitly representing these errors in the formulation, (13) becomes

$$\Delta P_{k\text{-}l} = \Delta P \Psi_{k\text{-}l} + e. \tag{14}$$

B. LSE-Based Algorithms for ISF Computation

We discuss three measurement-based algorithms to obtain an estimate of $\Psi_{k\text{-}l}$ by solving the overdetermined system in (14). The first is the conventional LSE solution, followed by WLS estimation, which weights certain measurements more than others. Finally, we describe the recursive least-squares (RLS) algorithm, which allows us to refine the ISF estimate as more measurements are obtained.

1) Least-Squares Estimation: We can obtain the least-squares estimate of the ISF vector for line $L_{k\text{-}l}$, $\Psi_{k\text{-}l} = [\Psi_{k\text{-}l}^1, \ldots, \Psi_{k\text{-}l}^i, \ldots, \Psi_{k\text{-}l}^n]^T$, by solving the following LSE problem:

$$\min_{\Psi_{k\text{-}l}} e^T e. \tag{15}$$

The solution to this problem is given by (see, e.g., [16])

$$\hat{\Psi}_{k\text{-}l} = (\Delta P^T \Delta P)^{-1} \Delta P^T \Delta P_{k\text{-}l}. \tag{16}$$

In doing so, we make two key assumptions: (i) the ISFs are approximately constant across the $m + 1$ measurements, and (ii) the regressor matrix ΔP has full column rank.

2) Weighted Least-Squares Estimation: As stated previously, one of the assumptions we make in (15) is that the ISFs are approximately constant across the estimation time window. One way to eliminate this restriction and to obtain an estimator that is more adaptive to operating changes is to place more importance on recent measurements and less on earlier ones, which may be out-of-date due to possible operating point changes. Hence, we consider a WLS estimation problem setting in which the objective function in (15) becomes

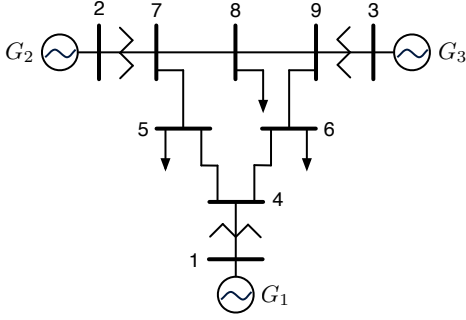$$\min_{\Psi_{k\text{-}l}} e^T W e, \tag{17}$$

Fig. 1: Network topology for WECC 3-machine 9-bus system.

where W is a positive definite symmetric matrix. The solution to (17) is given by (see, e.g., [16])

$$\hat{\Psi}_{k\text{-}l} = \left(\Delta P^T W \Delta P\right)^{-1} \Delta P^T W \Delta P_{k\text{-}l}. \qquad (18)$$

In our setting, the elements of the error vector e are uncorrelated; therefore the matrix $W = [w_{ij}]$ is diagonal. If the variations in $\Psi_{k\text{-}l}$ are slow compared to the dynamics of the system, the generic method is WLS with exponential forgetting factor [17], in which the more recent measurements are preferentially weighted by setting $w_{ii} = f^{m-i}$ for some fixed $f \in (0,1]$, where f is called a "forgetting" factor. If $f = 1$, then all measurements are given equal weighting, as in the conventional LSE objective function in (15). On the other hand, if $f < 1$, then earlier measurements would not contribute as much to the final estimate $\hat{\Psi}_{k\text{-}l}$ as more recent ones, i.e., earlier measurements are "forgotten" as more data is acquired [17]. This is especially useful for the case in which the system experiences a change in operating point during the time window in which measurements are obtained.

3) Recursive Least-Squares Estimation: In practical implementation, measurements would be obtained sequentially. Therefore, instead of waiting to collect a large dataset (and thus a longer period of time) before an estimate can be obtained, we use the RLS scheme to solve the estimation problem and update the estimate as more data is acquired [15]. As such, we consider one measurement set at a time, which consists of $\Delta P_{k\text{-}l}[j]$ and $\Delta P[j]$, the jth element of $\Delta P_{k\text{-}l}$ and the jth row of ΔP, respectively. Then, $\hat{\Psi}_{k\text{-}l}[j]$, the jth ISF estimate, can be obtained via the following recursive relation [15]:

$$\hat{\Psi}_{k\text{-}l}[j] = \hat{\Psi}_{k\text{-}l}[j-1] + Q^{-1}[j]\Delta P^T[j]$$
$$\left(\Delta P_{k\text{-}l}[j] - \Delta P[j]\hat{\Psi}_{k\text{-}l}[j-1]\right), \quad (19)$$

where $Q[j] = fQ[j-1] + \Delta P^T[j]\Delta P[j]$ and $Q[0] = \delta I$, δ small. Further, the computationally expensive matrix inversion in (19) may be avoided by invoking the Sherman Morrison formula (a special case of the matrix inversion lemma). Let $R[j] = Q^{-1}[j]$ and define so-called *gain vector* as

$$g[j] = \frac{1}{f + \Delta P[j]R[j-1]\Delta P^T[j]}R[j-1]\Delta P^T[j]. \quad (20)$$

TABLE I: Comparison of ISFs obtained for Example 1.

Line	Actual [p.u.] Before	After	Model-based [p.u.] Before/After	WLS Estimation [p.u.] $f=1$	$f=0.7$
$\Delta P_{4\text{-}5}$	-0.2970	-0.2046	-0.3196	-0.2145	-0.2203
$\Delta P_{4\text{-}6}$	-0.1734	-0.1426	-0.1804	-0.0529	-0.1416
$\Delta P_{7\text{-}8}$	+0.1838	+0.2121	+0.1804	+0.1116	+0.2066

Then, $\hat{\Psi}_{k\text{-}l}[j]$ can be obtained via the following recursive relation [15]:

$$\hat{\Psi}_{k\text{-}l}[j] = \hat{\Psi}_{k\text{-}l}[j-1] + R[j]\Delta P^T[j]$$
$$\left(\Delta P_{k\text{-}l}[j] - \Delta P[j]\hat{\Psi}_{k\text{-}l}[j-1]\right), \quad (21)$$

where $R[j] = f^{-1}\left(R[j-1] - g[j]\Delta P[j]R[j-1]\right)$ and $R[0] = \delta^{-1}I$.

Next, we illustrate the ideas presented above on LSE-based solutions to the overdetermined system in (14) via an example.

Example 1 (3-Machine 9-Bus System): In this example, we consider the WECC 3-machine, 9-bus system model (see, e.g., [18]), the topology for which is shown in Fig. 1. In order to simulate PMU measurements of slight fluctuations in active power injection at each bus, we synthetically generate power injection times-series data. To this end, we assume the injection at bus i, denoted by P_i, can be modeled as

$$P_i[j] = P_i^0[j] + \sigma_1 P_i^0[j]v_1 + \sigma_2 v_2, \quad (22)$$

where $P_i^0[j]$ is the nominal power injection at bus i at instant j, and v_1 and v_2 are pseudorandom values drawn from standard normal distributions with 0-mean and standard deviations $\sigma_1 = 0.1$ and $\sigma_2 = 0.1$, respectively. The first component of variation, $\sigma_1 P_i^0[j]v_1$, represents the inherent fluctuations in generation and load, while the second component, $\sigma_2 v_2$, represents random measurement noise. In addition, in order to capture the effect of a change in operating point, the active load at Bus 6 linearly increases by 2.8 p.u. over the span of 120 measurements, beginning at time instant $j = 180$, with the generation at Bus 2 also increasing commensurately by an equal amount at each time step. We assume this change is undetected to highlight the value of the proposed measurement-based method.

For each set of bus injection data, we compute the power flow, with the slack bus absorbing all power imbalances, and the active power flow through each line for that particular time. Suppose a 0.5 p.u. increase is applied to G_2 at bus 2 with the slack bus absorbing the resulting power imbalance. Table I shows a comparison between the corresponding effect on three lines computed from the actual power flow solution (both before and after the change in operating point), the linearized DC model-based approximation, and a solution to our measurement-based method using the recursive implementation of WLS in (21), with forgetting factors $f = 1$ and $f = 0.7$. Both measurement-based estimations are executed at time instant $j = 600$ with the previous $m = 600$ measurement sets. Since the operating point change is undetected by operators, the model-based ISF estimate is computed using the system model prior to the change. Note that the model-based estimations remain constant for operating point changes caused by varying load/generation. So the model-based estimates in Table I are also valid after the operating point change.
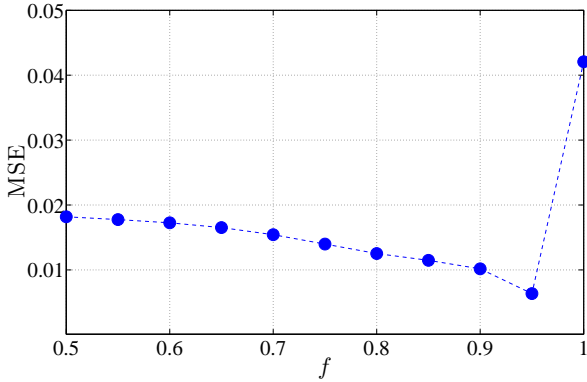
Fig. 2: Sensitivity of MSE to forgetting factor value in 3-machine 9-bus system.

TABLE II: Comparison of ISFs obtained for Example 3.

Line	Actual [p.u.]	WLS Estimation [p.u.]			
		$j = 300$	$j = 400$	$j = 500$	$j = 600$
$\Delta P_{4\text{-}5}$	-0.2970	-0.0685	-0.2683	-0.2974	-0.3017
$\Delta P_{4\text{-}6}$	-0.1734	-0.0567	-0.1758	-0.1730	-0.1747
$\Delta P_{7\text{-}8}$	+0.1838	0.0395	0.1204	0.1781	0.1831
$\vdots$	$\vdots$	$\vdots$	$\vdots$	$\vdots$	$\vdots$
MSE	—	0.6742	0.1265	0.0132	0.0086

Columns 2 and 3 in Table I depict the changes in line flows due to a 0.5 p.u. generation increase in G_2 before and after the operating point change, respectively. It is evident from Table I that the recursive WLS estimation scheme (column 5) with $f = 0.7$ is able to track the ISFs after operating point change with significant higher accuracy than both the model-based approach and the conventional LSE with $f = 1$. ∎

C. On Selection of the Forgetting Factor

There have been numerous proposed techniques to vary the forgetting factor f in RLS (see, e.g., [19], [20]) in time-varying systems. For example, we can vary f by monitoring the error residual variance $e^2[j]$, where $e[j] = \Delta P_{k\text{-}l}[j] - \Delta P[j]\hat{\Psi}_{k\text{-}l}[j]$ at each time instant j; when $e^2[j]$ increases, f is decreased [19]. Intuitively, if the error is small, then either the system has not undergone any changes or the estimated ISFs correspond closely to the changes that it has undergone. In either case, a reasonable strategy is to retain as much past information as possible by choosing f close to unity. On the other hand, if the error is large, then f should be chosen to be smaller so as to shorten the effective memory of the estimator until ISFs are readjusted and errors are small.

In general, when the forgetting factor is close to 1, RLS achieves low misadjustment (roughly the noise in the resulting estimate) and good stability, at the cost of reduced tracking capability. On the other hand, tracking capability is improved with a smaller forgetting factor, but misadjustment increases and stability may be affected [20]. Since the thrust of the current work is to propose a measurement-based approach to compute ISFs, instead of focusing on the optimal choice of a variable forgetting factor, we use a well-chosen constant f (via, e.g., a sensitivity study to determine the value of f that results in least estimation error) for each of the examples and case studies to highlight the potential of our proposed approach. Next, we present a sensitivity study with respect to the choice of constant f via an example involving the WECC 3-machine 9-bus system.

Example 2 (3-Machine 9-Bus System): In this example, we consider the same system and contingency scenario as in Example 1 and perform the ISF computation for a range of

$f \in [0.5, 1]$. For each value of f, we compare the resulting predicted flow through all lines to the actual post-contingency flows and compute the mean squared error (MSE). As shown in Fig. 2, the optimal f, which results in the smallest MSE, is around 0.95. In fact, a more granular sensitivity study done for $f \in [0.9, 1]$ shows that the optimal f in for this scenario is 0.97. This sensitivity study indicates that the forgetting factor should be chosen to be fairly close to 1. ∎

D. On Managing Bad Data

PMU data may contain random errors arising from equipment limitations in the measurement device and communication devices [21]. Detection and identification of bad data are commonly performed after an estimate has been computed by processing the measurement residuals, using schemes such as the χ^2-test and hypothesis testing, respectively [21]. Some bad data, such as (i) negative voltage magnitudes, (ii) values that are orders of magnitude too large or too small, and (iii) vastly different currents in and out of a bus, can be removed prior to ISF computation based on plausibility checks [21]. In this paper, we assume standard plausibility tests have been applied to the PMU measurements before they are passed to the LSE-based algorithms for ISF estimation. Moreover, the effect of bad data can be reduced or eliminated by (i) setting the forgetting factor to be smaller so that earlier, possibly erroneous, data have less influence on the ISF estimation; and (ii) conducting estimation over a sliding window in time so that any erroneous data eventually become ineffectual as more recent measurements are acquired.

Example 3 (3-Machine 9-Bus System): In this example, we consider the same system as in Example 1, but with constant operating point. We simulate 600 sets of measurements of slight fluctuations in bus injections and compute the corresponding line flows. We also inject additional random measurement error with zero mean and $\sigma = 0.5$ from time instant $j = 201$ to $j = 300$, without modifying the line flow measurements accordingly. We estimate ISFs at 4 time instants, $j = 300, 400, 500, 600$, using the previous 300 measurements and with $f = 0.97$. Suppose the injection at bus 2 increases by 0.5 p.u., Table II shows the predicted real power flow through a subset of lines due to this change as well as the MSE of all predictions as compared to the actual quantities (shown in column 2) obtained by solving the nonlinear power flow. As is apparent from the MSEs in Table II, the predictions become more accurate as new data is acquired and previous bad data are "forgotten", until the effects of the bad data are entirely eliminated in the final column with $j = 600$. ∎

E. Computation of Other Distribution Factors

Once the ISFs are obtained via online estimation, we can compute other relevant linear sensitivity DFs. Next, we describe the algorithm to obtain PTDFs, LODFs, followed by OTDFs.

1) Power Transfer Distribution Factor: The PTDF, denoted by $\Phi_{k\text{-}l}^{ij}$, approximates the sensitivity of the active power flow in line $L_{k\text{-}l}$ with respect to an active power transfer of a given amount of power, ΔP_{ij}, from bus i to j [7]. The PTDF can be computed as a superposition of an injection at bus i and a withdrawal at bus j, where the slack bus accounts for the power imbalance in each case. Thus,

$$\Phi_{k\text{-}l}^{ij} = \Psi_{k\text{-}l}^i - \Psi_{k\text{-}l}^j, \tag{23}$$

where $\Psi_{k\text{-}l}^i$ and $\Psi_{k\text{-}l}^j$ are the line flow sensitivities in line $L_{k\text{-}l}$ with respect to injections at buses i and j, respectively.

2) Line Outage Distribution Factor: The LODF, denoted by $\Xi_{k\text{-}l}^{k'\text{-}l'}$, approximates the active power flow change in line $L_{k\text{-}l}$ due to the outage of line $L_{k'\text{-}l'}$ as a percentage of pre-outage active power flow through $L_{k'\text{-}l'}$ [7]. Then, $\Xi_{k\text{-}l}^{k'\text{-}l'}$ is expressed as

$$\Xi_{k\text{-}l}^{k'\text{-}l'} = \frac{\Phi_{k\text{-}l}^{k'l'}}{1 - \Phi_{k'\text{-}l'}^{k'l'}} = \frac{\Psi_{k\text{-}l}^{k'} - \Psi_{k\text{-}l}^{l'}}{1 - (\Psi_{k'\text{-}l'}^{k'} - \Psi_{k'\text{-}l'}^{l'})}. \tag{24}$$

3) Outage Transfer Distribution Factor: The OTDF, denoted by $\Gamma_{k\text{-}l,k'\text{-}l'}^{ij}$, approximates the sensitivity of the active power flow in line $L_{k\text{-}l}$ with respect to an active power transfer of a given amount of power, ΔP_{ij}, from bus i to j after the outage of line $L_{k'\text{-}l'}$ [7]. Then $\Gamma_{k\text{-}l,k'\text{-}l'}^{ij}$ is expressed as

$$\Gamma_{k\text{-}l,k'\text{-}l'}^{ij} = \Phi_{k\text{-}l}^{ij} + \Xi_{k\text{-}l}^{k'\text{-}l'} \Phi_{k'\text{-}l'}^{ij}. \tag{25}$$

In the special case that bus j is the slack bus, (25) simplifies to

$$\Gamma_{k\text{-}l,k'\text{-}l'}^{i} = \Psi_{k\text{-}l}^{i} + \Xi_{k\text{-}l}^{k'\text{-}l'} \Psi_{k'\text{-}l'}^{i}. \tag{26}$$

IV. APPLICATIONS OF MEASUREMENT-BASED DISTRIBUTION FACTOR ESTIMATION

As stated previously, DFs are utilized in numerous power system monitoring and protection applications. In this section, we describe and formulate the role of measurement-based
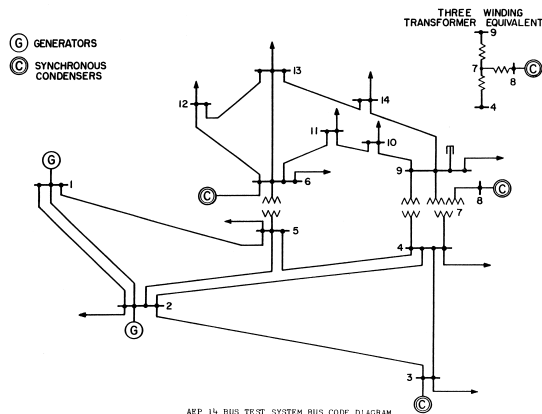
DFs in contingency analysis and generation re-dispatch in a security-constrained system. We illustrate the advantage of our measurement-based method over the model-based one in these applications through several examples. For all case studies discussed in Sections IV and V, we generate synthetic PMU measurements of power injections at each bus in the system by using (22) in Example 1. For each set of bus injection data, the active power flow through each transmission line is computed to simulate line flow measurements.

A. Contingency Analysis

To maintain power system security, operators must ensure that the system remains operable with the outage of any single asset (such as a generating unit or transmission line) at all times. In general, the procedure involves modeling all "credible" outages, one scenario at a time, and checking all lines and voltages in the network against their respective limits [3]. This exhaustive procedure is repeated regularly throughout the day as up-to-date measurements are procured and, due to constantly changing system conditions, results must be generated quickly to ensure operators are aware of any potential violations. If a power flow model of the system is available, one way to gain solution speed in contingency analysis is to use DFs under the DC power flow assumptions as described in Section II-A. In particular, we describe the role of DFs in contingency analysis in the following.

1) Generator Outage Contingency: For ease of notation, we assume there is at most one generator at each bus or that multiple generators at one bus have been lumped into one equivalent generator. In the event that an outage of a large generator, which had been generating P_i^0 (which corresponds to active power flow of $P_{k\text{-}l}^0$ in line $L_{k\text{-}l}$ in the pre-contingency state), occurs, the change in P_i would be

$$\Delta P_i = -P_i^0.$$

Suppose the loss of the generator at bus i were compensated by governor action on other generators throughout the interconnected system. Denote the proportion of ΔP_i that is compensated by the jth generator as β_j. Then, using ISFs, the post-contingency flow on line $L_{k\text{-}l}$ can be computed as

$$P_{k\text{-}l} = P_{k\text{-}l}^0 + \Psi_{k\text{-}l}^i \Delta P_i - \sum_{j \in \mathcal{B}, j \neq i} \Psi_{k\text{-}l}^j \beta_j \Delta P_i, \tag{27}$$

where $0 \leq \beta_j \leq 1$ and $\sum_{j \in \mathcal{B}, j \neq i} \beta_j = 1$. This computation is carried out for all lines $L_{k\text{-}l} \in \mathcal{L}$, and corresponding line flow limits $P_{k\text{-}l}^{\max}$ are checked to alarm power system operators to potential overloads. A common mechanism to assign values to β_j is to assume the remaining generators pick up the loss of the generator at bus i in proportion to their maximum MW rating as follows (see, e.g., [3]):

$$\beta_j = \frac{P_j^{\max}}{\sum_{k \in \mathcal{B}, k \neq i} P_k^{\max}}. \tag{28}$$

In the case that the slack bus (bus 1) is assumed to compensate for all lost generation due to the generator outage at bus i, in (27), we set $\beta_1 = 1$ and $\beta_j = 0$ for all $j \neq 1$.

Fig. 3: Network topology for IEEE 14-bus system [22].

TABLE III: Contingency analysis on 14-bus system with G_2 outage.

Line $L_{k\text{-}l}$	Pre-contingency $P^0_{k\text{-}l}$ [p.u.]	Post-contingency $P_{k\text{-}l}$ [p.u.] Actual	Model-based	Measurement-based
$L_{1\text{-}2}$	1.5674	1.9228	1.9008	1.9226
$L_{1\text{-}5}$	0.7587	0.8281	0.8253	0.8287
$L_{2\text{-}3}$	0.7285	0.7173	0.7172	0.7177
$L_{2\text{-}4}$	0.5601	0.5365	0.5366	0.5371
$L_{2\text{-}5}$	0.4190	0.3871	0.3872	0.3877
$L_{3\text{-}4}$	-0.2367	-0.2472	-0.2480	-0.2471
$L_{4\text{-}5}$	-0.5953	-0.6263	-0.6282	-0.6265
$\vdots$	$\vdots$	$\vdots$	$\vdots$	$\vdots$
MSE	—	—	0.0222	0.003

TABLE IV: Contingency analysis on modified 14-bus system with outage in $L_{4\text{-}5}$.

Line $L_{k\text{-}l}$	Pre-contingency [p.u.] $P^0_{k\text{-}l}$	$\tilde{P}^0_{k\text{-}l}$	Post-contingency $P_{k\text{-}l}$ [p.u.] Actual	Model-based	Measurement-based $f=1$	Measurement-based $f=0.8$
$L_{1\text{-}2}$	1.5674	1.5684	1.8004	1.7492	1.8170	1.7946
$L_{1\text{-}5}$	0.7587	0.7582	0.5610	0.5774	0.5840	0.5629
$L_{2\text{-}3}$	0.7285	0.7295	0.9065	0.8803	0.9035	0.9017
$L_{2\text{-}4}$	0.5601	0.5617	0.9268	0.8751	0.9149	0.9128
$L_{2\text{-}5}$	0.4190	0.4172	0.0933	0.1339	0.1231	0.1065
$L_{3\text{-}4}$	-0.2367	-0.2358	-0.0717	-0.0850	-0.0749	-0.0767
$L_{4\text{-}5}$	-0.5953	-0.6124	—	—	—	—
$\vdots$	$\vdots$	$\vdots$	$\vdots$	$\vdots$	$\vdots$	$\vdots$
MSE	—	—	—	0.1878	0.0538	0.0465

Example 4 (IEEE 14-Bus System): In this example, we consider the benchmark IEEE 14-bus system from [22], the topology of which is shown in Fig. 3. We examine the contingency where the system loses the generator G_2 due to an outage, with the generator G_1 picking up any resulting power imbalance, i.e., $\beta_1 = 1$ and $\beta_j = 0$ for all $j \neq 1, 2$. In the pre-contingency state, $P^0_2 = 0.4$ p.u. and, so to consider the outage of G_2, we set $\Delta P_2 = -0.4$ p.u. Table III shows the pre-contingency and post-contingency flows from the full power flow solution, the model-based approach, and the proposed measurement-based approach for a subset of transmission lines in the system. As Table III shows, the proposed measurement-based approach provides more accurate post-contingency flows than the model-based. In fact, the MSE for the post-contingency flows through all lines obtained via the model-based approach is 0.0222, whereas the measurement-based approach yields a MSE of 0.003. We will illustrate in Example 5 that the proposed measurement-based method is especially advantageous over the conventional model-based approach for a case in which the system topology or operating point has changed, unbeknownst to system operators. ∎

2) Line Outage Contingency: LODFs indicate the portion of pre-outage flow in a line, after its outage, that is redistributed onto remaining lines. Suppose in the pre-contingency state, the active power flow in lines $L_{k\text{-}l}$ and $L_{k'\text{-}l'}$ are $P^0_{k\text{-}l}$ and $P^0_{k'\text{-}l'}$, respectively. Furthermore, consider a contingency in which an outage occurs in line $L_{k'\text{-}l'}$; then, the post-contingency flow in $L_{k\text{-}l}$, using LODFs in (24), can be computed as

$$P_{k\text{-}l} = P^0_{k\text{-}l} + \Xi^{k'\text{-}l'}_{k\text{-}l} P^0_{k'\text{-}l'}. \tag{29}$$

Similar to the loss of generator study, the computation in (29) is repeated for all lines $L_{k\text{-}l} \in \mathcal{L}$. If no line constraints are violated with any single line outage, we conclude the system is N-1 secure with respect to line outages.

Example 5 (IEEE 14-Bus System): In this example, we begin with the same base case system as in Example 4, the line flows for which are denoted by $P^0_{k\text{-}l}$ (see Table IV). We consider a time window that contains $m = 600$ sets of pseudo-measurements obtained via randomly perturbing the active power injections at each bus. Suppose a line outage occurs in $L_{10\text{-}11}$, unbeknownst to system operators at sample $j = 100$, perhaps because it is located in a neighboring balancing area. Due to this undetected outage, the line flows become $\tilde{P}^0_{k\text{-}l}$ as shown in the same table. Contingency analysis continues to be conducted on the system using the LODFs

computed based on the model of the original system, which is no longer accurate due to the undetected $L_{10\text{-}11}$ outage. For the modified system, we present contingency analysis results for the hypothetical case in which line $L_{4\text{-}5}$ fails in Table IV (columns 4–7). More specifically, we compare between pre- and post-contingency (of $L_{4\text{-}5}$) actual line flows, model-based computed line flows, and measurement-based estimated line flows. The post-contingency flows based on linear DFs (shown in columns 5–7) are obtained as

$$P_{k\text{-}l} = \tilde{P}^0_{k\text{-}l} + \Xi^{4\text{-}5}_{k\text{-}l} \tilde{P}^0_{4\text{-}5},$$

with $\Xi^{4\text{-}5}_{k\text{-}l}$ as given by the model-based or the measurement-based approach, as appropriate.

By inspecting Table IV, which contains active power flow data for a subset of the transmission lines in the 14-bus system, we note that the measurement-based estimates are, on average, more accurate than the model-based ones. By setting the forgetting factor to $f = 0.8$, we are able to further refine the LSE estimates to reflect the current system topology. The MSEs are 0.1878, 0.0538, and 0.0465 for the post-contingency flows through all lines obtained via the model-based approach, LSE-based approach with $f = 1$, and LSE-based approach with $f = 0.8$, respectively. This example highlights one of the major advantages of the proposed measurement-based method, which, unlike the conventional model-based approach, automatically adapts to the current system topology and operating point. ∎

B. Generation Re-Dispatch

Suppose the contingency analysis from Section IV-A resulted in one or more violations of transmission line flow limits in the event of a "credible" outage. For example, following the outage of line $L_{k'\text{-}l'}$, suppose the post-contingency active power flow in line $L_{k\text{-}l}$, $P_{k\text{-}l}$, exceeds the maximum allowable power transfer of $P^{\max}_{k\text{-}l}$, rendering the system N-1 insecure. In this case, power system operators may dispatch out-of-merit generators, i.e., more expensive units, so as to correct the security violation. One way to achieve this is to solve a security-constrained optimal power flow on a model of the system with up-to-date measurements and state estimator results [23]. However, this method requires an accurate model that reflects current system topology and operating conditions. An alternative approach is to employ ISFs in conjunction with unit bid prices to select the most economical unit(s) to resolve the potential line flow violation in the event of the
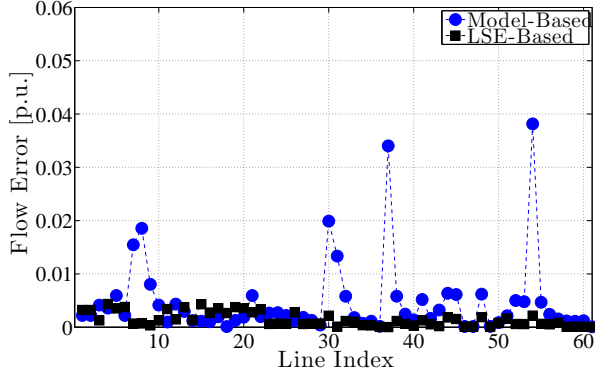
(a) Contingency analysis in the base case.
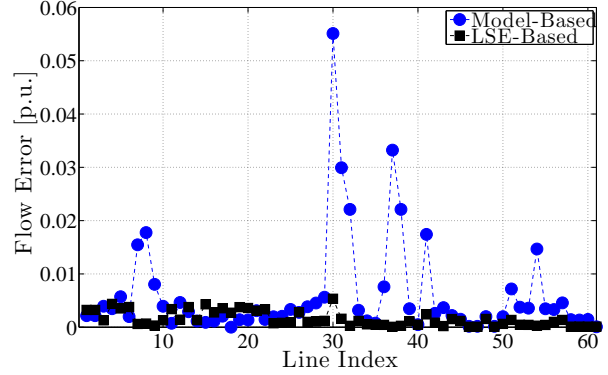
(b) Contingency analysis with modified external system.

Fig. 4: 118-bus system contingency analysis for G_{12} outage: comparison between deviations away from actual post-contingency flows resulting from the model- and measurement-based approaches.

corresponding contingency. The formulation of this alternative approach, which is used by, e.g., PJM [24], is summarized next.

Let $\bar{\gamma}$ denote the dispatch rate determined by the economic dispatch solution, where generator i with bid γ_i is dispatched to meet the electricity demand if $\gamma_i \leq \bar{\gamma}$. Suppose the most recent contingency analysis reveals that the system is not N-1 secure, with active power flow in line $L_{k\text{-}l}$ at risk of overload. Let ρ_i denote the so-called "$/MW effect" for unit i, where

$$\rho_i := \frac{\bar{\gamma} - \gamma_i}{\Psi_{k\text{-}l}^i}. \tag{30}$$

With the constraint on $P_{k\text{-}l}$, the unit with the lowest ρ_i is re-dispatched to relieve the violation. The generation re-dispatch for unit i^*, with the lowest ρ_i among all candidate generators, is computed using OTDFs in (26) as

$$\Delta P_{i^*} = \Gamma_{k\text{-}l,k'\text{-}l'}^{i^*} \left(P_{k\text{-}l}^{\max} - P_{k\text{-}l} \right). \tag{31}$$

Unlike the previous applications, we defer illustrating the advantage of our proposed method over the model-based one for this application to the next section.

V. CASE STUDIES

In this section, we use the proposed measurement-based DF estimation approach in the IEEE 118-bus system for the applications to contingency analysis and generation re-dispatch described in Section IV. The simulation tool MATPOWER [18] is used throughout to compute relevant transmission line flow measurements from pseudo-random bus injections. The system is divided into two zones, where zone 1 consists of buses indexed by $\mathcal{B}_1 = \{1 - 40, 113, 114, 115, 117\}$ and zone 2 consists of buses with indices $\mathcal{B}_2 = \{41 - 112, 116, 118\}$. In particular, we consider zone 1 as the internal system, whereas zone 2 is a neighboring balancing area (external system) whose operating point or topology changes may not be reported to the internal system operator in a timely fashion so as to allow zone 1 to adjust its network model accordingly. Through the case studies, we show that the pre-calculated model-based DFs may not be accurate if the system operating point and

network topology deviate sufficiently far away from those at which the sensitivity factors were computed, while the proposed measurement-based approach is able to adapt to system changes. Since PTDFs are relatively insensitive to bus injections and withdrawals if the topology is fixed [8], we focus on undetected topology changes, such as line outages, in the external system to highlight the value of the proposed measurement-based approach to contingency analysis.

On the computational time: For all case studies in this section involving the IEEE 118-bus system, we compute ISFs using a time window that contains $m = 500$ sets of measurements. On average, to obtain the ISFs of line $L_{k\text{-}l}$ with respect to all buses, denoted by $\Psi_{k\text{-}l}$, requires 0.1505 s. For comparison, the standard LSE, as described in Section III-B1, requires an average of 0.00225 s to compute $\Psi_{k\text{-}l}$ using the same set of measurement data. It is also worth noting that the computation for $\Psi_{k\text{-}l}$ can be done in parallel with ISFs of any other line $\Psi_{k'\text{-}l'}$.

A. Generator Outage Contingency

In this case study, we consider the outage of the generator at bus 12, denoted by G_{12}, as the candidate contingency under two scenarios. In both, we validate the proposed measurement-based approach by comparing post-contingency line flows obtained via full nonlinear power flow solution and model- and measurement-based ISF computations. After the G_{12} outage, the pre-contingency generation is divided among three neighboring generators, G_{10}, G_{25}, and G_{26}, with the proportions dictated by their maximum MW ratings as in (28).

1) Base Case: We assume the time window under consideration contains $m = 500$ sets of measurements. As in Example 1, the bus injection data P_i are simulated by adding noise to the nominal value P_i^0 as given in (22), with $\sigma_1 = \sigma_2 = 0.01$. We obtain the benchmark post-contingency flows for all lines in the internal system $\mathcal{B}_1$ by solving the nonlinear power flow with the outage and re-distribution of pre-outage power generation of G_{12}. Figure 4a shows the deviation of the post-contingency flows obtained via model- and measurement-based approaches from the actual quantities for lines in the

TABLE V: Actual pre- and post-contingency line flows in 118-bus system.

Line	Pre-contingency		Post-contingency
$L_{k\text{-}l}$	$P_{k\text{-}l}^0$ [p.u.]	$\tilde{P}_{k\text{-}l}^0$ [p.u.]	$P_{k\text{-}l}$ [p.u.]
$L_{23\text{-}24}$	0.0828	0.0189	0.0344
$L_{26\text{-}30}$	2.2371	2.2624	2.2564
$L_{23\text{-}32}$	0.9298	0.9519	0.9465
$L_{15\text{-}33}$	0.0731	0.1004	0.0930
$L_{33\text{-}37}$	-0.1572	-0.1301	-0.1374
$L_{34\text{-}36}$	0.3025	0.3115	0.3088
$L_{34\text{-}37}$	-0.9431	-0.8590	-0.8849
$L_{38\text{-}37}$	2.4337	2.6851	2.6145
$L_{37\text{-}39}$	0.5491	0.7380	1.2548
$L_{37\text{-}40}$	0.4402	0.6236	—

TABLE VI: Comparison of post-contingency flows in 118-bus system with undetected outages in $L_{41\text{-}42}$ and $L_{42\text{-}49}$.

Line	Actual	Model-based	Measurement-based [p.u.]		
			$j = 500$		$j = 800$
$L_{k\text{-}l}$	[p.u.]	[p.u.]	$f = 1$	$f = 0.98$	$f = 1$
$L_{23\text{-}24}$	0.0344	0.0497	0.0523	0.0296	0.0360
$L_{26\text{-}30}$	2.2564	2.2509	2.2499	2.2589	2.2564
$L_{23\text{-}32}$	0.9465	0.9410	0.9402	0.9481	0.9459
$L_{15\text{-}33}$	0.0930	0.0860	0.0842	0.0933	0.0908
$L_{33\text{-}37}$	-0.1374	-0.1445	-0.1462	-0.1372	-0.1396
$L_{34\text{-}36}$	0.3088	0.3066	0.3064	0.3093	0.3085
$L_{34\text{-}37}$	-0.8849	-0.9049	-0.9125	-0.8855	-0.8928
$L_{38\text{-}37}$	2.6145	2.5585	2.5446	2.6274	2.6052
$L_{37\text{-}39}$	1.2548	1.1697	1.1451	1.2673	1.2346
$L_{37\text{-}40}$	—	—	—	—	—
$\vdots$	$\vdots$	$\vdots$	$\vdots$	$\vdots$	$\vdots$
MSE	—	0.1187	0.1650	0.0287	0.0266

internal system. The measurement-based approach yields, on average, more accurate results than the model-based one. In fact, the MSE for the model-based solution is 0.0066, whereas the measurement-based approach yields a MSE of 0.0015.

2) Modified External System: Suppose line outages have occurred for $L_{65\text{-}68}$ and $L_{47\text{-}69}$, which are both in the external system, unbeknownst to the internal system operators. Again, we collect $m = 500$ sets of measurements from the modified system, where the simulated bus injection data consist of load/generation fluctuations with $\sigma_1 = 0.01$, and measurement noise with $\sigma_2 = 0.01$. Again, we compare the errors resulting from the model- and measurement-based approaches against the benchmark nonlinear power flow solution in Fig. 4b. By visual inspection, we note that the errors in some line flows increase for the model-based approach, while they remain similar to the base case for the measurement-based approach. In fact, the MSE for the post-contingency flows obtained via the model-based approach increases to 0.0086, while those obtained via the measurement-based approach yields a MSE of 0.0015 still. Additionally, we also computed ISFs by linearizing the AC power flow model, as $-cJ^{-1}D$ in (7). The MSE for the post-contingency flows obtained via the AC-model-based approach is about equal to those obtained via the measurement-based approach. Therefore, we conclude that the error yielded by the measurement-based method is mostly due to error inherent to the linearization process.

B. Line Outage Contingency

Here, we consider the outage of line $L_{37\text{-}40}$ in the internal system as the candidate in contingency analysis. We begin with the original base case system at time $j = 1$. Suppose, at time $j = 200$, outages occur in lines $L_{41\text{-}42}$ and $L_{42\text{-}49}$ in the external system. We solve the full nonlinear power flow and obtain the active line flows in the base case system (denoted by $P_{k\text{-}l}^0$), the modified system with undetected outages in the external area (denoted by $\tilde{P}_{k\text{-}l}^0$), and the post-contingency modified system with the additional outage of line $L_{37\text{-}40}$ (denoted by $P_{k\text{-}l}$). The resulting power flows through a subset of internal system transmission lines are shown in Table V.

In Table VI, we reproduce the actual post-contingency flows from Table V in column 2. Using the pre-contingency flows for the modified system, $\tilde{P}_{k\text{-}l}^0$, and the LODFs computed from the base case system topology, the model-based post-contingency flows are computed and shown in column 3 of Table VI. The MSE for the post-contingency flows through

all internal system transmission lines obtained via the model-based approach is 0.1187.

Suppose at time $j = 500$, contingency analysis is conducted using the previous $m = 500$ sets of measurements, which includes the loss of external lines at $j = 200$. As in Section V-A, the simulated bus injection data consist of load/generation fluctuations with $\sigma_1 = \sigma_2 = 0.01$. Using simulated bus injection and line flow data, we estimate ISFs and compute LODFs with forgetting factors $f = 1$ and $f = 0.98$, the post-contingency flows for which are listed in columns 4 and 5 in Table VI, respectively. While the unweighted LSE produces post-contingency flows that are similar to the model-based computation, weighted LSE with $f = 0.98$ matches the actual post-contingency line flows quite well, as shown in Table VI. In fact, the MSE for the post-contingency internal system line flows obtained via unweighted LSE is 0.1650, while those obtained via the weighted LSE yields a MSE of 0.0287. For comparison, suppose the same contingency analysis is performed at time $j = 800$, using the previous $m = 500$ sets of measurements, during which the topology does not change further since the previous external system line outages. The post-contingency flows resulting from estimation of ISFs using unweighted conventional LSE are shown in column 6 of Table VI. Again, these computations match the actual post-contingency flow well and the MSE for the post-contingency internal system line flows is 0.0266 in this case.

C. Generation Re-Dispatch

In this case study, we consider the outage of transformer between buses 37 and 38, denoted by $T_{37\text{-}38}$, as the candidate contingency with undetected external system outage of lines $L_{41\text{-}42}$ and $L_{42\text{-}49}$. Using the same set of measurement data as contingency analysis performed at $j = 800$ from Section V-B, we illustrate the advantage of the proposed measurement-based approach over the model-based one.

For this case study, we use the generator cost data available in the 118-bus MATPOWER case. Upon performing economic dispatch, we find the dispatch rate to be $\overline{\gamma} = \$39.38$/MWh. With the undetected external system line outages, we conduct contingency analysis with the hypothetical $T_{37\text{-}38}$ outage, with the real power flow through line $L_{15\text{-}33}$ summarized in Table VII. Next, suppose that the thermal limit of line

TABLE VII: Contingency analysis on modified 118-bus system with outage in $T_{37\text{-}38}$.

Line	Pre-contingency [p.u.]		Post-contingency $P_{k\text{-}l}$ [p.u.]		
$L_{k\text{-}l}$	$P_{k\text{-}l}^0$	$\tilde{P}_{k\text{-}l}^0$	Actual	Model-based	Meas-based
$L_{15\text{-}33}$	0.0470	0.0752	1.0378	0.9001	1.0742

TABLE VIII: Choosing generator to relieve $L_{15\text{-}33}$ overload on modified 118-bus system with outage $T_{37\text{-}38}$.

G_i	γ_i [$/MWh]	ISF $\Psi_{15\text{-}33}^i$		ρ_i [$/MW Effect]	
		Model-based	Meas-based	Model-based	Meas-based
G_{34}	40.05	-0.0627	-0.0620	10.6688	10.7909
G_{36}	40.10	-0.0650	-0.0666	11.0480	10.7933
G_{40}	40.00	-0.0566	-0.0707	10.9217	8.7546

TABLE IX: Comparison of model- and measurement-based approaches to relieve $L_{15\text{-}33}$ overload on modified 118-bus system with outage $T_{37\text{-}38}$.

Approach	G_{i*}	ΔP_{i*} [MW]	$P_{15\text{-}33}$ [p.u.]	Cost [$/hr]
Model	G_{34}	32.55	0.9365	1314
Meas	G_{40}	25.55	0.9604	1028

$L_{15\text{-}33}$ is 1 p.u. Then the system is not N-1 secure under the $T_{37\text{-}38}$ contingency. Note that while the measurement-based method flags this violation, the model-based computation is unable to do so. Based on the ISFs for line $L_{15\text{-}33}$, there are three out-of-merit generators in zone 1—G_{34}, G_{36}, and G_{40}—that can be dispatched to relieve the thermal overload. By applying (30) to these generators, using both the model- and measurement-based ISFs, we obtain the value of ρ_i for each unit (see Table VIII). According to the computation of ρ_i done with the model-based ISFs, G_{34} should be used to relieve the constraint on line $L_{15\text{-}33}$, whereas the computation using the measurement-based ISFs dictates that G_{40} ought to be dispatched. The cost functions for these generators are $C(P_{34}) = 0.01P_{34}^2 + 40.05P_{34}$ and $C(P_{40}) = 0.01P_{40}^2 + 40.0P_{40}$. Table IX shows a comparison between the re-dispatch resulting from the model- versus measurement-based approaches using (31). Indeed, by solving the nonlinear power flow for both scenarios and the resulting total generation cost, while both scenarios relieve the post-contingency flow violation in line $L_{15\text{-}33}$, we confirm that the dispatch of G_{40} produces the lower cost.

VI. CONCLUDING REMARKS

In this paper, we presented a method to estimate DFs through LSE, which does not rely on the system power flow model, using PMU measurements collected in real-time. Beyond eliminating the power flow model, we show that the proposed measurement-based approach provides more accurate results than the model-based approximations and can adapt to unexpected system topology and operating point changes. Further, we improve the adaptability of the proposed technique by incorporating WLS and place more weight on recent measurements and less to past ones. We also implement the estimation scheme recursively so that ISF estimates are refined with each additional set of measurements obtained.

Further work includes analysis of the optimal choice for the forgetting factor in the context of LSE-based DF estimation and accurate estimation of DFs in the presence of corrupted measurements or the availability of only a subset of measurements. Also, the measurement-based method necessitates an over-determined system. Hence, an avenue for future work would be to devise algorithms that estimate the DFs accurately using fewer measurements.

REFERENCES

[1] FERC and NERC. (2012, Apr.) Arizona-southern california outages on september 8, 2011: Causes and recommendations. [Online]. Available: http://www.ferc.gov/legal/staff-reports/04-27-2012-ferc-nerc-report.pdf
[2] U.S.-Canada Power System Outage Task Force. (2004, Apr.) Final report on the august 14th blackout in the united states and canada: causes and recommendations. [Online]. Available: https://reports.energy.gov/BlackoutFinal-Web.pdf
[3] A. Wood and B. Wollenberg, *Power Generation, Operation and Control*. New York: Wiley, 1996.
[4] Z. Dong and P. Zhang, *Emerging Techniques in Power System Analysis*. Springer-Verlag, 2010.
[5] US DOE & FERC. (2006, Feb.) Steps to establish a real-time transmission monitoring system for transmission owners and operators within the eastern and western interconnections. [Online]. Available: http://energy.gov
[6] P. Sauer, "On the formulation of power distribution factors for linear load flow methods," *IEEE Transactions on Power App. Syst.*, vol. PAS-100, pp. 764–779, feb 1981.
[7] B. Stott, J. Jardim, and O. Alsac, "Dc power flow revisited," *IEEE Transactions on Power Systems*, vol. 24, no. 3, pp. 1290 – 1300, 2009.
[8] R. Baldick, "Variation of distribution factors with loading," *IEEE Transactions on Power Systems*, vol. 18, no. 4, pp. 1316–1323, 2003.
[9] T. Güler, G. Gross, and M. Liu, "Generalized line outage distribution factors," *Power Systems, IEEE Transactions on*, vol. 22, no. 2, pp. 879–881, 2007.
[10] J. Guo, Y. Fu, Z. Li, and M. Shahidehpour, "Direct calculation of line outage distribution factors," *IEEE Transactions on Power Systems*, vol. 24, no. 3, pp. 1633 – 1634, 2009.
[11] J. E. Tate and T. J. Overbye, "Line outage detection using phasor angle measurements," *IEEE Transactions on Power Systems*, vol. 23, no. 4, pp. 1644 – 1652, 2008.
[12] H. Zhu and G. B. Giannakis, "Sparse overcomplete representations for efficient identification of power line outages," *IEEE Transactions on Power Systems*, vol. 27, no. 4, pp. 2215 – 2224, 2012.
[13] E. B. Makram, M. C. Vutsinas, A. A. Girgis, and Z. Zhao, "Contingency analysis using synchrophasor measurements," *Electric Power Systems Research*, vol. 88, pp. 64 – 68, 2012.
[14] Y. C. Chen, A. D. Domínguez-García, and P. Sauer, "Online computation of power system linear sensitivity distribution factors," in *Proc. of the IREP Bulk Power System Dynamics and Control Symposium*, August 2013.
[15] S. Haykin, *Adaptive Filter Theory*. Prentice Hall, 1996.
[16] F. Schweppe, *Uncertain Dynamic Systems*. Englewood Cliffs, NJ: Prentice-Hall Inc., 1973.
[17] L. Ljung and T. Söderström, *Theory and practice of recursive identification*. MIT Press, 1983.
[18] R. D. Zimmerman, C. E. Murillo-Snchez, and R. J. Thomas, "Matpower: Steady-state operations, planning and analysis tools for power systems research and education," *IEEE Transactions on Power Systems*, vol. 26, no. 1, pp. 12–19, feb 2011.
[19] L. Ljung and S. Gunnarsson, "Adaptation and tracking in system identification - a survey," *Automatica*, vol. 26, no. 1, pp. 7 – 21, 1990.
[20] C. Paleologu, J. Benesty, and S. Ciochina, "A robust variable forgetting factor recursive least-squares algorithm for system identification," *Signal Processing Letters, IEEE*, vol. 15, pp. 597 –600, 2008.
[21] A. Abur and A. G. Exposito, *Power System State Estimation: Theory and Implementation*. Marcel Dekker, 2004.
[22] University of Washington. (2012, Oct.) Power system test case archive. [Online]. Available: http://www.ee.washington.edu/research/pstca/
[23] A. Monticelli, M. V. F. Pereira, and S. Granville, "Security-constrained optimal power flow with post-contingency corrective rescheduling," *IEEE Transactions on Power Systems*, vol. 2, no. 1, pp. 175–180, 1987.
[24] PJM State & Member Training Department. (2012, October) Transmission operating criteria. [Online]. Available: https://pjm.com